Marine Geology xxx (xxxx) xxx–xxx

Contents lists available at ScienceDirect

Marine Geology

journal homepage: www.elsevier.com/locate/margo

A new chalcolithic-era tsunami event identified in the offshore sedimentary record of Jisr al-Zarka (Israel)

Natalia Tyuleneva[a,b], Yael Braun[a], Timor Katz[c], Igor Suchkov[b], Beverly Goodman-Tchernov[a,*]

[a] University of Haifa, Mt. Carmel, Israel
[b] Odessa I. I. Mechnikov National University, Ukraine
[c] Israel Oceanographic and Limnological Research Institute, Shikmona, Israel

ARTICLE INFO

Keywords:
Tsunami
Coastal sediments
Clay minerals
XRD
XRF
FT-IR
Chalcolithic

ABSTRACT

Tsunami field evidence is a critical resource for determining coastal risk. However, in many cases there is low potential for long term preservation of such deposits on land. A growing body of evidence suggests that tsunami deposits can be present in the shallow offshore realm and may present a largely untapped, but important worldwide sedimentological reference set for investigating past tsunami events. Here, different proxies for tsunami sediment identification and differentiation (granulometry, XRD, XRF, FT-IR) were used to determine the presence or absence of such deposits in a core collected offshore at Jisr al-Zarka, midway between Tel Aviv and Haifa. The study aimed to recognize anomalous deposits and test different analytical methods to define their origins. Five anomalous sedimentological horizons were identified, four of which were interpreted as tsunamigenic by comparison to previously identified poorly sorted, shell-rich tsunamites found nearby in Caesarea and contrast to the fine-sand, Nile-derived background sediments. The remaining anomaly was distinctive, but not determined to be tsunamigenic due to a lack of coarse shell in the matrix. The oldest tsunamigenic layer, coinciding with the Chalcholithic cultural period (5.7 ka), is the oldest such deposit identified offshore Israel to date and the non-tsunamigenic anomalous horizon may correspond with a transitional climatic phase (~5.5 ka). This research reinforces the importance of offshore investigations as a means of improving tsunami catalogues and identifying environment-altering events.

1. Introduction

1.1. Offshore deposits

The potential for using offshore, shallow shelf sedimentary deposits as a record of short term and long term events, such as those caused by extreme storms, floods, tsunamis, and environmental transitions is being widely explored (Feldens et al., 2009, 2012; Goto et al., 2012; Ikehara et al., 2014; Katz et al., 2015; Kitahashi et al., 2014; Sakuna et al., 2012).

In the case of offshore Israel, the lack of information regarding these deposits results primarily from the complications of collection in the sandy sediments, where > 50 cm long cores is only possible with commercial drilling rigs, in which resolution is severely compromised, or recently developed diver-assisted methods (Goodman-Tchernov et al., 2009) as were used in this study. Here, a range of analysis were performed on a newly collected and previously collected cores to reconstruct past events which impacted the area now populated by the village of Jisr al-Zarka.

1.2. Tsunami deposits

Tsunami events can result in unusual, anomalous depositional sequences, which in certain circumstances are preserved and can be distinguished from typical background deposits. These tsunami-generated layers have been recognized not only in sedimentary sections in nearshore and coastal environments, but also in the shallow shelf (Dawson and Stewart, 2007; De Martini et al., 2010; Goodman-Tchernov et al., 2009; Goodman Tchernov et al., 2016; Papadopoulos et al., 2014; Smedile et al., 2012; van den Bergh et al., 2003; Veerasingam et al., 2014). Existing proxies used for the identification of such abrupt and rare hazardous events as tsunamis differ and vary across study sites, primarily due to the range of characteristics of marine and terrestrial sediment sources, as well as local topography and geology (Dawson and Stewart, 2007; Font et al., 2011; Goff et al., 2012). As a result, the character of tsunami deposits can vary widely, and there is ample need and motivation to consider and test different proxies and describe different examples. Amongst the great challenges in tsunami studies is differentiating tsunami deposits from other depositional events such as

* Corresponding author.
E-mail address: bgoodman@univ.haifa.ac.il (B. Goodman-Tchernov).

http://dx.doi.org/10.1016/j.margeo.2017.07.008
Received 21 August 2016; Received in revised form 9 July 2017; Accepted 12 July 2017

storms or floods, and the related challenge of determining the best areas for discovering and identifying previously unidentified event horizons. The latter issue is complicated by differences in preservation potential.

The study of tsunami deposits in the geological record requires a detailed analysis of the sedimentary sequences preceding, during, and after events as a means to produce a non-event reference set, or typical 'background' conditions for comparison. This is especially necessary since considerable amounts of both marine and terrestrial material are mobilized and displaced during tsunami events, thus creating a variety of sediment signatures. Generally, tsunami deposits are recognized when certain conditions are met, particularly the presence of a laterally continuous, allochthonous, anomalous occurrence in an otherwise predictable or well-defined sedimentological setting, which cannot be explained by other events. Many of the first seminal works on tsunami deposits concentrated on marine signatures identified in very well-constrained terrestrial settings, such as coastal fresh-water lake sediment sequences (Bondevik et al., 1997; Clague et al., 2000; Dawson and Shi, 2000; Hutchinson et al., 1997; Minoura et al., 1994; Sawai et al., 2008). These deposits are ideal, as they leave little room for doubt regarding the source of the material and its allochtonous provenance. Also, since terrestrial deposits are clearly preferred as they might also provide critical information for reconstructing run-up and inundation minimums, these studies set the standard for many years. However, not all coastlines are coincident with these features. Also, many deposits left on land immediately following the event do not necessarily remain long-term. Recent repeated surveys of nearshore terrestrial tsunami deposits from the 2004 Indian Ocean-Sumatra Tsunami suggest that erasure of many of the deposits can occur in a relatively short time frame. For example, 70% of deposits recorded in the month succeeding the event were not visible 5 years later (Szczuciński, 2012). Within paleostudies, the suggestion was raised that shallow offshore marine sediments might yield even more information about paleotsunamies than terrestrial deposits (Reinhardt et al., 2006; Rhodes et al., 2006). Since then, this prediction was supported with new field and modeling evidence (Bintanja et al., 2005; Feldens et al., 2009; Goodman-Tchernov and Austin, 2015; Goodman Tchernov et al., 2016; Paris et al., 2010; Sakuna et al., 2012; Srinivasalu et al., 2010; Weiss and Bahlburg, 2006).

1.3. Identifying tsunami layers offshore

In some circumstances tsunami deposits can be better preserved offshore since they are less affected than onshore tsunami deposits by surface processes, tectonic movements and anthropogenic alteration; particularly in occupied or urbanized areas with systematic and thorough post-event clean-ups (Dey et al., 2014; Spiske et al., 2013; Szczuciński, 2012). Observations following recent tsunamis suggest that the amount of sediment movement and bathymetric change that occurs in the offshore is substantial (Feldens et al., 2009, 2012; Goto et al., 2011), and that sediment-laden currents with the potential for initiating turbidites can also be observed(Ikehara et al., 2014). On the continental shelf of the Andaman Sea, in depths ranging between 9.5 and 15.9 m below sea level and 2.9 to 7.2 km offshore; distinguishable layers associated to flashfloods, major storms, and tsunamis are visible in gravity cores (Sakuna-Schwartz et al., 2015). It has been noted that while a diverse set of characteristics are recognizable in association to post-tsunami offshore deposits and morphological changes (Mamo et al., 2009), their long-term preservation potential (Kitahashi et al., 2014) as well as uniqueness relative to storm influence may be problematic (Milker et al., 2013). Nearly all of the research to date emphasizes the importance of the local conditions (geology, coastal and offshore bathymetry/topography, sedimentation regime, vegetation, etc.) and it is regularly noted that no single indicator serves as a standalone means to define tsunamigenic sediments (Goff et al., 2012; Sakuna et al., 2012; Shanmugam, 2012). Therefore, studies rely on a multitude of approaches and proxies to recognize and define tsunami deposits.

Offshore from Caesarea, for example, cores retrieved from a water depth of 14.3 to 20 m below mean sea level contain at least three anomalous layers defined as tsunamigenic (Dey and Goodman-Tchernov, 2010; Goodman-Tchernov et al., 2009). Amongst the tsunami indicators include debris of archaeological artifacts, poor sorting and changing distribution of the sediments (both size and shape), imbricated mollusk shells, microfossil assemblage transitions, and more; in stark contrast to the relatively homogenous Nile-derived sand horizons that deposit during non-event conditions. Continued work on these deposits is demonstrating their usefulness for reconstructing the impact of the events and introducing new ways of recognizing the horizons, such as the association made via geophysics sub-bottom chirp survey between shallow water ancient marine installations and backwash channeling in the underlying sedimentary deposits (Goodman-Tchernov and Austin, 2015). The work at Caesarea, especially due to the convenient high contrast between Nile-derived background sediments and the tsunami horizons, provides a useful baseline experimental site for searching for additional tsunami deposits in other areas along this coastline as well as testing various analytical proxies.

In recent years the toolkit for tsunami identification has been considerably expanded and improved (Chagué-Goff et al., 2012; Goff et al., 2012), and comparisons of offshore and onshore records have been presented (Dey et al., 2014; Smedile et al., 2012; Tipmanee et al., 2012). Certain approaches are proving to be uniquely beneficial in the offshore, such as shallow geophysical surveys (high resolution pre/post event bathymetry, sub-bottom mapping); particularly when combined with coring and historical data (Abrantes et al., 2005; Goodman-Tchernov and Austin, 2015; Paris et al., 2010; Smedile et al., 2012; van den Bergh et al., 2003). Approaching the offshore analysis, like any environmental analysis, requires that attention must be paid to the specific circumstances. For example, a layer of significant abundance of marine foraminifera (of any species) in a freshwater body is supportive of a marine water incursion, and with other supporting evidence could be used to identify the layer as a tsunami event. Offshore, the mere presence of foraminifera is not sufficient, but rather the unique assemblage, condition, or size of the foraminifera (Goodman Tchernov et al., 2016; Pilarczyk and Reinhardt, 2012; Smedile et al., 2012). Broadly, site-specific indicators of the offshore must be assessed just as any environmentally-specific characteristics that ultimately provide support for movement, redeposition, and a means to recognize original provenance and differentiate from other influences such as storms and floods.

Fourier Transform Infrared spectroscopy (FT-IR), as a means to determine mineralogical composition, is being acknowledged as an efficient provenance identification tool. FT-IR was previously used to discriminate between marine sediments and accumulated tsunami backwash deposits (Pongpiachan et al., 2013). It was also applied to produce offshore mineralogical measurements (Veerasingam et al., 2014) that distinguished between terrestrial and marine sediment sources.

Heavy minerals can potentially be used for sediment provenance and hydrodynamic pattern identification; such as those expected from tsunami events because they tend to concentrate in laminae following high energy events (Babu et al., 2007; Cascalho et al., 2016; Chagué-Goff et al., 2012; Costa et al., 2012; Jagodziński et al., 2009; Nakamura et al., 2012). For example, studies of tsunami signatures after the 2004 Indian Ocean Sumatra Tsunami completed on the southeastern Indian coast (Srinivasalu et al., 2010) demonstrated a distinct shift in sediments offshore immediately following the tsunami event.

In recent years XRF analysis has been used as an efficient approach for paleo-environmental reconstructions including identification of tsunami events (Abrantes et al., 2008; Font et al., 2011; Minoura et al., 2000). Marine and lake sedimentary records are widely studied using this method, providing data about composition of chemical elements used for deciphering changes in depositional settings through time and

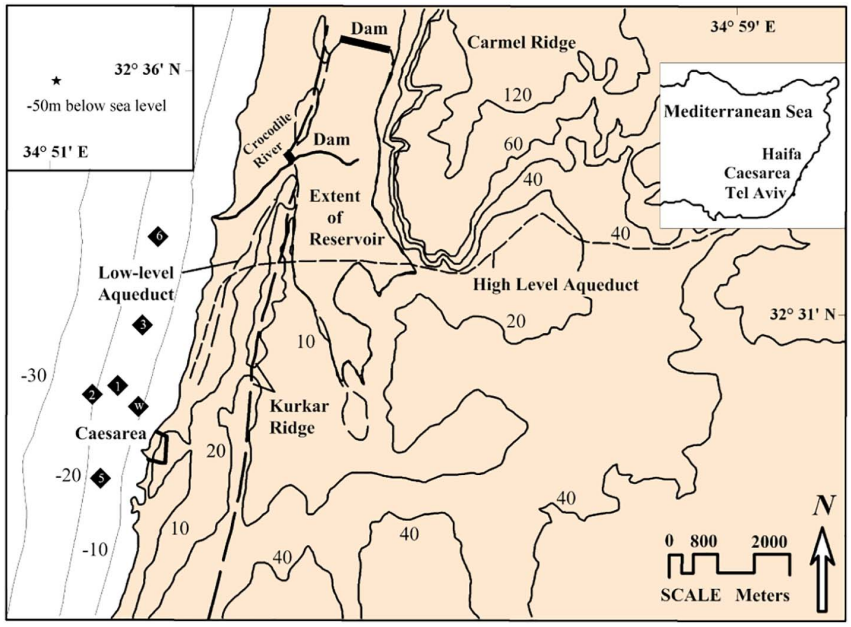

Fig. 1. A) Topographic map of the study area, depicting the Crocodile River position, aqueducts, dams, and Carmel Ridge in central Israel (adapted from Reinhardt et al., 2003); B) Location map of sediment cores offshore Caesarea and Jisr al-Zarka: 1–3, 5, 6 (marked as black hexagons) and Area W underwater excavation (marked as a black square), isobaths are in meters. A surface sample from − 50 m below sea level was also collected and is indicated by the * within the upper left inset.

space (Boyle, 2000; Löwemark et al., 2011; Martín-Puertas et al., 2011).

Changes of sedimentological setting under the influence of tsunamis on onshore areas where alluvial systems are developed are well known and observed in different parts of the world (Hindson and Andrade, 1999; Srinivasalu et al., 2009; Young et al., 1996) as well as studies of redistribution of coastal deposits and formation of offshore submarine accumulative relief forms (Gianfreda et al., 2001). At the same time, not much is known about the resetting of offshore alluvial systems under the impact of tsunami waves.

The study presented here focuses on the identification of sedimentological indicators in comparison with normal marine depositional patterns. Analyses on these samples were carried out in the same procedure as previous studies in Caesarea for comparative purposes, and newer analyses was added (Goodman-Tchernov et al., 2009). Thus, our research questions are to investigate the presence or absence of tsunami horizons or other anomalous horizons offshore from the village of Jisr al-Zarka, and test different analytical approaches to determine their usefulness (Fig. 1).

2. Regional setting

Jisr al-Zarka is a small village located 5 km north of Caesarea, near the archaeological remains of Krocodeilonopolis (Stieglitz, 1998, Fig. 1). The Crocodile River (Nahal Taninim, Fig. 1) originates in the Eocene and Cretaceous chalk and limestone hills to the east and then drains through the southern part of Mount Carmel, passes across the coastal plain, and finally cuts through the shore-parallel eolianite ridge (Horowitz, 1979). The Crocodile River cannot migrate significantly since it is constrained by a natural calcareous eolian sandstone ridge (Lichter et al., 2011, see Fig. 1) locally referred to as 'kurkar'. Kurkar is interbedded with extensive layers of loam - a soil composed of sand, silt, clay and organic matter, likely marshy zones that once existed between the shifting dune system. The sequence of eolianite and loam are present along the entire coastal plain and the continental shelf of Israel (Frechen et al., 2004; Goldsmith and Golik, 1980; Zviely et al., 2007).

The width of the shelf off the outflow of the Crocodile River is about 13.5 km, with a gentle gradient to 40 m, similar to other areas of Israel's continental shelf (Garfunkel, 1998; Neev et al., 1987). The sediments in the Kabara marshes are composed of silt and calcarenite which are within the silty-sandy grain size (Marco et al., 2014). Crocodile River sediments are dominated by sandy mud with clay content (Avnaim-Katav et al., 2016; Stanley et al., 1998). The area is part of the 650 km long, Nile littoral Cell (Inman and Jenkins, 1984) and is dominated by well-sorted siliciclastic quartz sands (120–160 μm), derived from the Nile drainage basin. At − 5 m to − 30 m water depths (Almagor, 2005). Another main component of sediments in this region is carbonaceous sand derived either from biogenic material, namely shell fragments or from eroded limestones and dolomites that outcrop the mountains to the east. These sediments are transported along the Israeli shoreline from the Nile Delta by a generally counter-clockwise longshore current (Goldsmith and Golik, 1980; Zviely et al., 2007). The net transport across the entire bottom profile (a band about 500 m wide) affected by all breaking waves, runs to the north (Zviely et al., 2007); though within the narrow band within 100 m from the shore, net transport sometimes runs to the south (Emery and Bentor, 1960; Perlin and Kit, 2002). According to Zviely et al. (2007) sand transport direction along the coast of Israel has not changed significantly during the past 8000 years, though Sivan et al. (2001, 2004) argues that some tectonic movement and sea-level change have occurred within this timeframe, which would have an impact on this system; though this would not necessarily have impacted the sources and directional trends. Therefore, Nile-derived sandy sediments are the primary source for both the modern offshore sediments as well as the older deposits.

Consequently, the present study also focused on the mineralogical composition of silt and clay (< 63 μm) rather than the dominant sand fraction, with the aim to capture clay minerals with specific sources. The first source is the Nile River, which supplies mostly smectite (Venkatarathnam and Ryan, 1971), the second is desert-derived dust of eolian origin, which carries kaolinite from the Sinai Peninsula (Stanley et al., 1998); the third brings clay minerals from the Israeli coast together with the sediments from the local streams (Jaffe et al., 2012; Sandler and Herut, 2000). The composition of the latter source varies, and the studies of sediments from the streams showed dominance of kaolinite on the Sinai and southern part of Mediterranean coast of Israel; smectite (S), illite (I) and kaolinite (Ka) in the central and northern parts (Stanley et al., 1998). The ratio of clay minerals in the nearby Crocodile River (Fig. 1) is S 78%, I 9% and Ka 13% (Stanley et al., 1998). Based on previous research (Stanley et al., 1998; Sandler and Herut, 2000), the assumption that smectite, illite, chlorite and kaolinite

constitute about 100% of clay minerals in the sediments is generally accepted.

Amongst the potential high energy events at the study site are storms, floods, earthquakes, and tsunamis. Catastrophic flood events significantly affect fluvial environment in semiarid and Mediterranean climates (Inbar, 2000). Winter rains are usually strong and fall over short time periods, occasionally resulting in floods (Horowitz, 1979). There are no direct hydrographic measurements from the Crocodile River, but on the entire coast, there are on average three to six floods per year, with mean daily flow higher than 4 m^3/s (Lichter et al., 2011). Storm records are incomplete for this area, with available instrumentally recorded data limited to the past decade. In 2010, a major storm consisted of 14 m wave height amplitudes from a station offshore at 25 m water depth (Katz and Mushkin, 2013). Damage was recorded on the coastline, but associated offshore deposits were not recorded.

The study area is characterized by low levels of seismic activity during the last decades (Mart and Perecman, 1996), though historical records show that the territory of Levant was affected by numerous strong earthquakes in the last 2.5 ka (Amiran et al., 1994). The Dead Sea rift (a transform boundary with left lateral displacement), the Sinai Negev shear zone and the Mount Carmel fault system (both dip-slip and strike-slip segments) are the main structures that shape the tectonics of Israel (Shapira and Hofstetter, 1993). Nearest to Jisr al-Zarka lies the Binyamina-Or Akiva segment, a deeply buried east-west normal fault. It is generally considered quiet or inactive, although a 4.2 Mw earthquake was recorded in 2014 approximately 40 km offshore. Tsunami waves can be generated directly from earthquakes or from submarine landslides (Salamon et al., 2011). Studies in Caesarea harbor gave evidence for both natural hazards, earthquakes and tsunamis, which damaged the ancient harbor in the 2nd century AD (Reinhardt et al., 2006) It is also suggested that in 749 CE a devastating earthquake destroyed the ancient city of Beit Shean in northern Israel (Amiran et al., 1994) and may have produced tsunami waves (Dey et al., 2014; Goodman-Tchernov and Austin, 2015). Injected sand liquefaction flame features in the reservoir deposits at Jisr al-Zarka were interpreted as related to seiche patterns that could have been associated to a tsunami event in the 18th century (Marco et al., 2014). Sedimentological environment in the proximal part of the eastern Mediterranean shelf was affected by sea-level changes and, in places by tectonic activity as well (Sivan et al., 2001). However, Caesarea and its coastal plain were structurally stable in the last 2000 years (Goodman-Tchernov and Katz, 2016). Sea level is considered relatively stable for the past two to four thousand years (Sivan et al., 2004, 2001).

3. Materials and methods

Samples for the study were subsampled from both newly collected cores and archived samples from previously studied cores. The newly collected cores included a 2.19 m long sediment core (C6) collected from 15.3 m below mean sea level, 1.5 km southwest of the Crocodile River (Fig. 1). The core was collected using a diver-operated percussion corer (methods in (Goodman-Tchernov et al., 2009). After extraction, the core was split, described, documented, photographed and sampled at 1 cm intervals. Granulometry, mineralogical studies, x-ray diffraction (XRD), x-ray fluorescence (XRF) and Fourier transform infrared spectroscopy (FT-IR) were performed. A second sample, collected using a piston corer, was collected from 50 m water depth, at a position situated approximately 12 km to the northwest of the mouth of the Crocodile River (32.606617° N; 34.860533° E). A surface sample from this core was prepared for XRD determination of the composition of clay minerals, as well as for grain size analysis in order to compare to deeper water sediments. Subsamples from previously studied Caesarea cores 1 and 2 (Goodman-Tchernov et al., 2009) were sampled for analyses. Samples were selected with the aim of targeting defined strata based on the previous interpretation and current study's granulometry and core descriptions. Ages for core 6 horizons were determined using radiocarbon-14 dating. While marine shells are problematic for radiocarbon-14 generally (Mangerud, 1972) they were preferred in this study for a few reasons. First, alternative short-lived organic candidates that reflect atmospheric carbon values (seeds, twigs, etc.) are rarely available. Secondly, articulated bivalves are expected to be reliably close to their death position, as disarticulation is common during post mortem transport, as is evident from the bivalves visible today in Israel on many beaches (Sivan et al., 2006). Thirdly, bulk sediment ages are problematic in these depths because of low carbon values overall, and erosional hiatus commonly present in association to the tsunami events. Lastly, previous studies nearby (Goodman-Tchernov et al., 2009; Reinhardt et al., 2006) also relied on these materials, and therefore correlation could also be done based on pre-calibration values, thereby removing some of the uncertainties of calibration for purposes of comparison. Radiocarbon dates were corrected for marine reservoir effect and converted to calendar years using CALIB 7.0.1 (http://calib.qub.ac.uk/calib/, Stuiver and Reimer, 1993). Methods for grain size analysis and contour mapping of the results followed (Goodman-Tchernov et al., 2009). A Rigaku MiniFlex 600 Benchtop X-ray diffractometer with a copper X-ray tube was used to study the mineralogy of the sediments of core 6. Settings were 15 mA and 40 kV, from 3 to 60° 2θ, at a scanning rate of 2° 2θ/min. Samples untreated, and samples saturated with dimethyl-sulfoxide (DMSO, (Garcia and Camazano, 1968) as well as a sample heated up to 600 °C for one hour, which were then studied to determine clay fraction composition.

Bulk sedimentary deposits were soaked in distilled water for 24 h to remove salts. Due to relatively low clay fraction content in core 6 (ca. 3%), a combined clay and silt fraction (< 63 μm) was obtained. For the same core an additional sample of the clay fraction was obtained using settling cylinders (1–5 μm) from the combined intervals (59–75 cm), which was necessary to achieve the minimum volume required for analysis. Sediments from the upper centimeter (0 to 1 cm) of piston core HL14P1 (50 m water depth) were very clay-rich (20 μm mean grain size) and therefore did not require special separation.

All samples were treated by a low-intensity ultrasonic treatment for a few minutes to extract as much of the clay fraction as possible. To prepare oriented samples the suspension from the upper layer was taken and a drop of suspended material was placed on a glass slide and left to dry in room temperature. After the first run, the same samples were placed in a desiccator with 2 ml of DMSO for 24 h and then were run again. Areas of the peaks in the samples saturated with DMSO were calculated and 17 Å is equal to a relative amount of smectite (S); the area under the 10 Å peak of illite was multiplied by 4; and 7 Å peak area which is characteristic for chlorite and kaolinite was multiplied by 2. Proportions of clay minerals in each sample were determined with purpose of most closely reflecting values present in nature (Biscaye, 1965; Pierce and Siegel, 1969).

Kaolinite and chlorite have similar basal spacing, which makes it difficult to distinguish between them since they are non-swelling minerals. Kaolinite, chlorite and swelling clay minerals were separated (Garcia and Camazano, 1968). It was expected to obtain expanded minerals of kaolinite after DMSO saturation and to get the basal reflection at 11.18 Å, though the characteristic bend within this range didn't appear. To distinguish between chlorite and kaolinite, an interval sample (from 59 to 75 cm) was heated up to 600 °C. At this point the bend at 7.13Å for untreated sample (Fig. 2), which shows the presence of both clay mineral chlorite and kaolinite, disappears. Absence of the basal reflection in that range after heating shows the dominance of kaolinite over chlorite, because the latter does not react to temperature treatment (Garcia and Camazano, 1968).

ED-XRF spectrometer (SPECTROSCOUT) was used for elemental analysis of homogenized sediment samples after removing the > 2 mm fraction, but otherwise following methods described previously (Rahav et al., 2016).

A study of bulk samples and their < 45 μm fraction was carried out

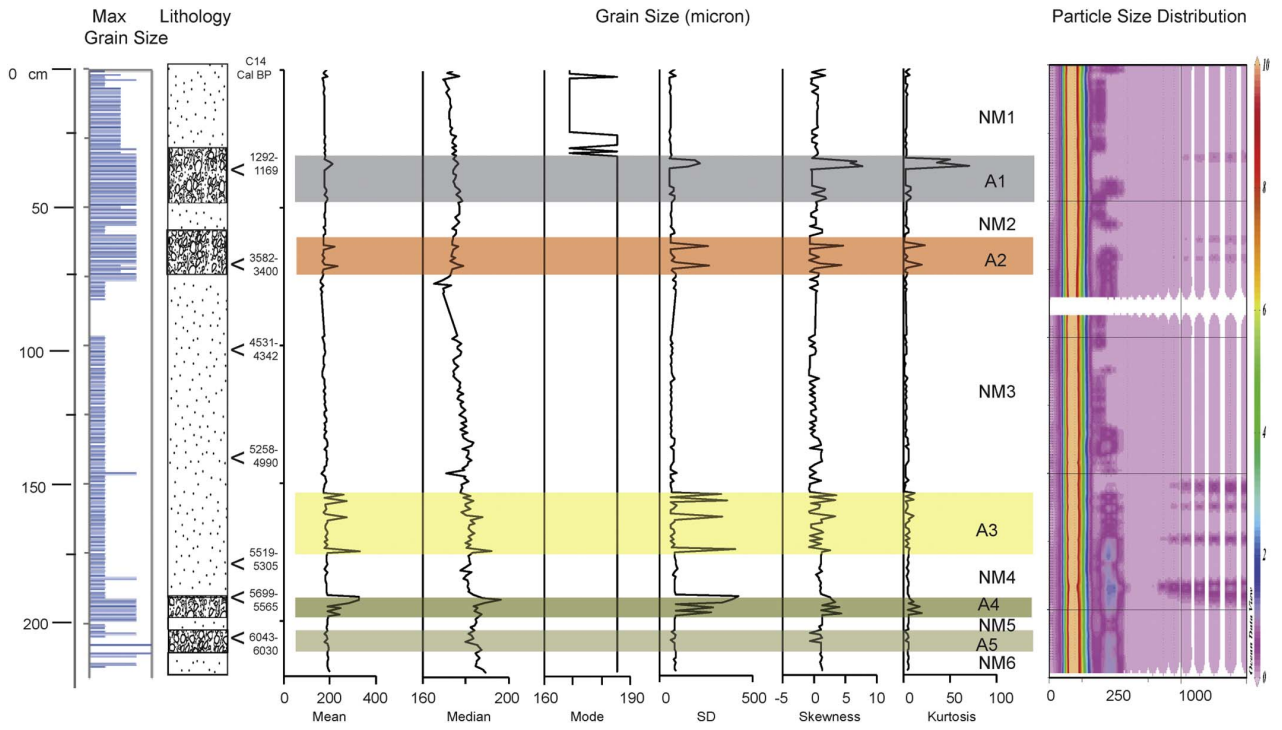

Fig. 2. Core 6 description and grain size analysis results. Grain size distribution analysis is displayed in a particle-size distribution contour map of the core. Data were plotted using Ocean Data View Software (version 3.3.2). NM 1–6 indicates 'normal' marine and A 1–5 anomalous environment of sedimentation. C - radiocarbon-14 ages, 2 calibration BP. Color code reflects the correlation with tsunamigenic sediments, identified previously in Caesarea (Goodman-Tchernov et al., 2009). (For interpretation of the references to color in this figure legend, the reader is referred to the web version of this article.)

Table 1
Radiocarbon-14 results.

Depth in core 6 (cm)	Analysis	Fraction of modern		Radiocarbon(BP), 1 σ error	2σ calibration	$\delta^{13}C$ per mil	Horizon	Material	Caesarea correlation
		pMC	1 σ error						
40–43	AMS	81.17	0.28	1675 ± 30	cal BP 1292to 1169	0	A1	Articulated bivalve *Glycymeris sp.*	E1
63–74	AMS	63.86	0.23	3600 ± 30	cal BP 3582to 3400	0	A2	Articulated bivalve *Glycymeris sp.*	E3
101–102	AMS	58.47	0.21	4310 ± 30	cal BP 4531 to4342	0	NM3	Articulated bivalve *Glycymeris sp.*	NM
143–144	AMS	54.89	0.26	4819 ± 38	cal BP 5258 to 4990	2.5	NM3	Articulated bivalve *Glycymeris sp.*	NM
180–181	AMS	53.28	0.23	5058 ± 35	cal BP 5519 to 5305	0.8	NM4	Articulated bivalve	NM
192–193	AMS	51.96	0.2	5259 ± 31	cal BP 5699 to 5565	2.3	A4	Gastropod	
210–211	AMS	48.98	0.2	5734 ± 33	cal BP 6043 to 6030	0.6	A5	Gastropod	

using a Fourier Transform Infrared Spectrometer (Nicolet Magna 860) and "Grams" software. A fraction was wet sieved through a 45 μm mesh screen, dried at 60 °C, homogenized in an agate mortar, treated with KBr, pressed into a disc, then dried at 150 °C. For especially clay-rich samples, a larger than aliquot of prepared sample was used to produce a 'concentrated' sample. These samples were analyzed to determine the ratio between clay minerals such as kaolinite (3697 cm^{-1}) and kaolinite and smectite (3620 cm^{-1}). Bulk samples were not separated nor dried (shell fragments were not included), but were analyzed to determine the ratio between Ca and Ar (1432 cm^{-1}) and quartz and clays (1082 cm^{-1}).

4. Results

4.1. Core 6: description granulometry, dating

After splitting the core, a description of visible characteristics was completed. The core is composed of a fine sandy matrix with four distinctive, shell and rubble rich horizons (Fig. 2) with sharp lower contacts. The maximum size of any inclusion was recorded before measuring the < 2000 μm grain size. The < 2000 μm grain size throughout core 6 is within the range of fine sand (mode 168–185, median 165–196, mean 125–250 μm (Udden, 1914; Wentworth, 1922)). The admixtures of silt (3.9–63 μm) and clay (0.37–3.8 μm) components on average were between near 3 to 18% (Fig. 2). While the

raw values vary, trends exist in the statistical values of Mean, Median, SD, skewness and kurtosis for horizons 'A1-A5' (Fig. 2); and intermediary horizons 'NM1–6' are more similar to each other than to A1-A5 (Figs. 2 and 4). In the upper part of the core (0-29 cm) the mode fluctuates but is mostly at a value of ~168 μm, while all horizons below are consistently around 185 μm (Fig. 2). In the ODV contour mapping, which is a representative tool to assist in highlighting changes in sorting for the < 2000 μm fraction, the 'A' and 'NM' layers are visible based on the presentation of increases in proportions of the larger size fraction within the 'A' layers, namely very coarse sand (1000–1821 μm). Samples for radiocarbon dating were selected based on these layers (Table 1).

Horizons NM1–6 characterized generally by matrix-supported, well-sorted fine sands. The mode grainsize value of NM1 (0–29 cm, present to ~1.2 ka BP) vacillates between 165 and 185 μm, while the mode values of NM2–6 are consistently 185 μm (Fig. 2).

Horizons A1 (29–49 cm, ~1.2 ka BP) contains gravel (round flint, eroded kurkar), *Glycymeris* and other shells (partial, fragmented, and sometimes articulated), embedded in the fine sand. Horizons A2 (59–75 cm, ~3.5 ka), A4 (191–199, ~5.6 ka), and A5 (203–211, ~6.0 ka) have similar grain size distributions and inclusions, with the highest concentration of framework-supported shell and rubble in A4 and A5. A layer of whole, imbricated *Glycymeris* shells is present in A4.

A3 (154–175 cm, ~5.2–5.4 ka BP) shares granulometric characteristics to the remaining 'A' horizons, but is devoid of > 5 mm shell, gravels, or small cobbles. The layer is differentiated by distinctive deviations in mean, SD, skewness and kurtosis (Figs. 2 and 4); and therefore, differed from both the normal marine horizons and the other anomalies. On average, it consists of fine sand of 83% and an admixture of medium sand of 4%. Maximum content of coarse and very coarse sand is between 2 and 10%.

4.2. XRD, XRF, FT-IR, minerology

4.2.1. XRD

The mineralogical composition of the clay fraction of nine samples from core 6 and a single sample from 50 m water depth was completed. The following assemblage of clay minerals was determined in the samples saturated with DMSO: smectite (S), hydromica (illite) (I), chlorite and kaolinite (Ch and Ka). Diffractograms of four samples, where the diffractogram of the surface sample from 50 m below mean sea level demonstrates the first order basal reflections at 18.35 Å of smectite, 10.01 Å of illite, 7.15 Å of kaolinite which coincided with the second order basal reflection of chlorite (Fig. 3).

XRD values in horizons NM1–6 are always < 60% for smectite, > 20% for Illite, and < 20% for Chlorite + Kaolinite (Fig. 5). The ratio of the determined clay minerals throughout core 6 varies (see Fig. 5) and differs significantly from the typical ratio of the comparative deeper water sample from 50 m water depth where the ratio of clay minerals is as follows for S 84%, I 3% and Ch and Ka 14%. A1, and the lower parts of A2 and A4 are characterized by a relative increase in chlorite and kaolinite content, where illite showed only some relatively higher content in A2 and A4 (Fig. 5). Overall, however, few strict trends were identified.

4.2.2. XRF

An assessment of relative chemical variations in lithological (Zr, Ti, Fe and Si) and biogenic (Ca and S) components of the deposits from both anomalous and normal marine settings was carried out for cores 1, 2 and 6 and the results are depicted in Fig. 6. Content of such elements as silica and calcium has an inverse relationship since they originate from two different sources, terrigenous and biogenic. Sediments of Caesarea's core 1 are characterized by three distinctive maximums of Ca content at 30 (E1), 91 (E3) and 160 cm depth. Titanium and zirconium along with such elements as iron and sulfur in the upper part of the core and at 140 cm have their maximum values. Sulfur has a considerably increased content at 91 and 140 cm, though this should be carefully assessed given the contribution of Sulfur in seawater generally.

Sediments from core 2 have three intervals with increased calcium content (50 cm:E2, 110 cm:E3, and 149 cm). Sulfur has two maximums, at 50 (E2) and 149 cm. Content of titanium and zirconium demonstrate similar tendencies as in core 1 (Fig. 6) with maximums in the upper part at 15 cm (E1) and downcore at 60 (E2), 120 (E3) and 149 cm. In general, iron repeats this tendency at the same intervals, excluding 60 cm.

Core 6 has increased values of Ca content in five intervals (37 cm:A1, 64 cm:A2, 130 cm:NM3, 194 cm:A4, 198 cm:A4 and 218 cm:NM6). Sulfur has increased values in intervals including 15 cm (NM1), 80 cm (NM3), 155 cm (A3), 165 cm (A3), 171 cm (A3) and 190 cm (NM4). The relative content variations of Ti, Fe and Zr show similar patterns (Fig. 6).

4.2.3. FT-IR

Variations of quartz, calcium carbonate as well as the ratio between kaolinite and smectite content were estimated. Conspicuous increments are not present (Fig. 7). Core 6 anomalies, such as A1, A2, and A4 showed kaolinite maximum relative values of 23, 21 and 22% respectively. Some tendencies in calcium carbonate content were noted in all studied cores. This component seems to become higher within anomalous horizons. Efforts were made to determine similarity or contrast between horizons through statistical comparisons as well as searching for trends, though none were recognized.

4.2.4. Mineralogy

The heavy minerals were isolated to determine the qualitative composition of samples and verify previous descriptions. The 250–90 μm fraction from the anomalous interval 198–199 cm in core 6 (A4, 1.98 g), was separated in heavy liquid (LST Heavy Liquid, 2.85 g/ml density), producing about 3% values for the heavy fraction. This quantity is significantly higher than the content of heavy fraction in the NM1 fraction 250–90 μm, where the sediment was separated with bromoform ($CHBr_3$) heavy liquid, with density of 2.89 g/ml, and after separation the weight of the heavy fraction was 1.7%. The mineralogical composition of both samples comprised of hornblende, augite, epidote, garnet, zircon, diopside, limonite, rutile, magnetite and apatite. Occasionally mica (biotite) was encountered. These data agreed with previously obtained results by Pomerancblum (1966).

5. Discussion

Analytical results from the offshore sediment core at Jisr al-Zarka resulted in the identification of eleven horizons, six of which are interpreted as typical background sediments, and five anomalous horizons, including four associated to tsunami-related deposits and one non-tsunamigenic. Interpretation of the horizons was determined by comparison to known typical background sediments and previously recognized tsunamigenic deposits. The main criteria used in previous studies nearby included granulometric parameters, shell content, and chronological constraints. In this study, these same parameters were used plus XRF, XRD, and F-TIR. Targeted subsamples (representative of background and tsunami horizons) were also measured from previously collected cores in Caesarea for comparison and correlation. They will be discussed here in chronological order, highlighting the anomalous horizons and their interpretations.

5.1. Chalcolithic-era anomaly

The oldest non-background anomalies are A4 (191–199 cm) and A5 (203 − 211), which may represent a previously unknown tsunami event or events (Fig. 8). It starts with a sharp contact at 211 cm. In this horizon, fine to medium sand with admixture of coarse sand was embedded with an imbricated shell layer, shell fragments, whole shells, gastropod shells in pristine condition, higher relative Ca values, a 3 cm

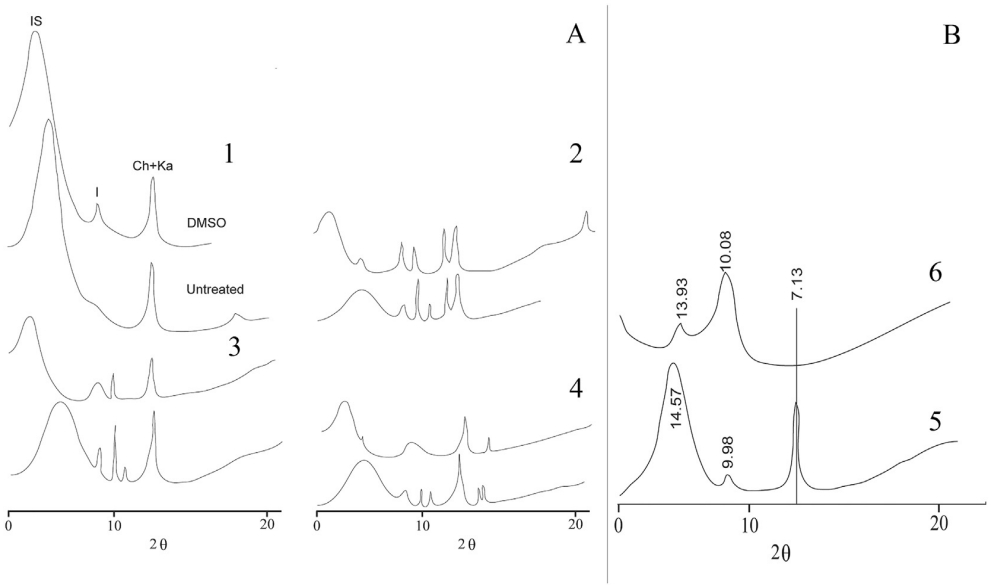

Fig. 3. A) X-ray diffractograms of typical samples: 1. Diffractograms of a surface sample from 50 m depth. Diffractograms of the core 6: 2. the combined interval from 40 to 41 cm, (ca. 749 CE); 3. the interval from 63 to 64 cm, A2 (ca. 3.5 ka BP); 4. the interval from 180 to 181 cm, NM 4 (ca. 5.5 ka BP). S- smectite, I – illite, Ch + Ka-chlorite and kaolinite. B) X-ray diffractograms of the combined interval 59–75 cm from core 6: 5. untreated sample; 6. heated sample under 600° for one hour.

fragment of eroded, worn calcareous sandstone covered with vermitid deposits at the base of the deposit, suggesting transport from the intertidal zone and then burial. The admixture of shell types likely reflects a combination of newly entrained, turbulent flow transported shells combined with older deposits from the coastline that were also eroded and suspended, ultimately resulting in this diverse combination. One possible explanation could be that it represents the intertidal zone itself, which is known to be mixed; however, according to sea level estimates for that time the horizon would be at the equivalent depth of around − 13 m (Fig. 8) which is still outside the tidal zone. A4 is preceded by a narrow band of 'normal' sedimentation (NM5), before a repeated layer of tsunamigenic-like sediments from 203 to 211 cm (A5). Given that there are two ages in reasonably close succession (5.6 ka BP in A4 and 6 ka in A5, see Table 1) it could suggest two events, or it is also possible that this is a sedimentary sequence from one event, as older ages within tsunami deposits are common due to the transport and redeposition of older materials. Importantly, whether one event or two, it represents the oldest coastal offshore tsunami layer/s identified so far in Israel or anywhere else in the Mediterranean.

Furthermore, the signatures from other methods showed that the deposits of A4 are characterized by increased values of Zr, Ti and Fe in the lower part of the sequence. According to the mineralogical analysis that was carried out for core 6 and other published data (Pomerancblum, 1966), these three elements which showed distinct and clear signals in the sedimentary record, are the main constituents of heavy minerals such as zircon, rutile, limonite, magnetite and hornblende. Heavy minerals are mainly concentrated in fine to medium sand fraction (63–250 μm), where the content of the latter reaches up to 87% for this interval. Minerals of the clay fraction could not significantly affect the results of the bulk samples analyzed here, because their quantity in the sediments of the A4 interval does not exceed 4%. The suggestion that higher concentrations of Zr, Ti and Fe in the lower part of the anomalous layer are attributed to heavy minerals was confirmed by the determination of their concentration in this specific interval. The content of heavy minerals from a representative sample of the non-tsunami layer in the upper part of the core (NM1) is 1.7%, which can be regarded as the background content of heavy minerals throughout the core, indicating normal marine sedimentation. The interval from 198 to 199 cm (A4) is characterized by the increase of heavy minerals content up to 3%. Therefore, it may be linked to the processes of mechanical concentration of heavy minerals. As it was shown in previous studies, Ti as well as Zr and Fe can be used as indicators of a high energy sedimentological environment (Cascalho et al., 2016; Chagué-Goff, 2010; Costa et al., 2015; Mahaney et al., 2016).

The newly identified tsunami, or two tsunamis, indicated in layers A4 and A5, occurred during the Chalcolithic ('Copper Age') cultural period of the region. Not surprisingly, there are no records for such an event, as the time period pre-dates historical tsunami and earthquake records. It was proposed that a Mount Etna eruption-sourced tsunami impacted the prehistoric site of Atlit Yam at around 8.3 ka BP, thus destroying the village and killing thousands (Pareschi et al., 2007). Their argument was based on the disturbed nature of the archaeological site and a reinterpretation of archaeological descriptions, and was not accepted by the site's excavators (Galili et al., 2008). This newly identified event (or events) in Jisr al-Zarka introduces the possibility that the ~5.6 ka/~6.0 ka 'A4/A5' event/s, and not an earlier Mt. Etna associated event, could be responsible for the alterations seen in Atlit Yam. By 6.0 ka Atlit Yam is expected to have already been abandoned, buried, and submerged due to sea-level rise (Galili et al., 2008, 1993) for at least one millenium, though it would have been in the more vulnerable, shallower depths. The ages proposed in Pareschi et al., 2007 are anchored in radiocarbon dates from dates published within the archaeological reports (Galili et al., 2008), which were selected for the specific purpose of determining the age of the archaeological remains. Galili pointed out the conflicts between these ages and the proposed Mt. Etna tsunami theory (Galili et al., 2008). A later tsunami, however, would better account for both the archaeological argument for the state of the remains showing signs of gradual abandonment and sea-level rise related disruption, as well as evidence of tsunami-related damage; albeit post-site abandonment.

5.2. Climate-associated anomaly

Above horizons A4/A5 there is a 16 cm-thick band of normal marine ('NM4') sediments and then an anomalous horizon A3 (see Figs. 2 and 8), which is distinctive due to grain size distribution and higher sedimentation rate. However, relative to the other anomalous layers in the core, it does not include larger inclusions (e.g. rubble, gravel, larger

whole shell or fragments) or mineralogical signatures, and therefore does not qualify as tsunamigenic as understood in this area. The estimated accumulated deposition rate is also on average > 50% than the overall rate calculated for the entire core (1.2 mm/yr versus 0.35 mm/yr). In addition, the horizon does not correspond with any previously identified tsunami events from nearby Caesarea. While intracore tsunami horizons could theoretically leave different signatures due to variations in the character of the tsunami (flow velocity, magnitude, directionality, source mechanism), changes in the environment, anthropogenic influence or post-depositional alterations, we do not think that it is the case. Our reasoning is that there are horizons interpreted as tsunamigenic present in other parts of the core, and we do not see these same changes repeated nor do we see such significant intracore variations between those horizons. For these reasons, this horizon is being excluded from the study's list of tsunami events.

The age of the anomaly can be bracketed between 5.2 and 5.5 ka, which coincides with a period of climate change, such as the termination of the African Humid Period that is also linked to higher sedimentation rates (Bar-Matthews et al., 1999; De Menocal, 2001; Lamy et al., 2006; Magny and Haas, 2004). The absence of larger inclusion sizes, which are common in the tsunamigenic layers also suggests that the increased sedimentation could be associated with increased river run-off, flooding, or other sediment input; but with less turbulent flow and shorter transport distances. The presence of increased sediment input, without the addition of a shell component is like comparative tsunami, storm, flashflood deposit observations offshore on the Adaman Sea continental shelf (Sakuna-Schwartz et al., 2015). There, background sediments from regular river discharge, with the most dominant being the Ayeyarwady–Salween river system, are in the silt-size range, storm and tsunami deposits were more poorly sorted and included a lower erosional contact, while floody deposits were finer and without the erosional contact. Similarly, in this study, anomaly A3 does not appear to have an erosional contact and the sedimentation rate is higher than the overall sediment rate in the core (see Figs. 2 and 4); making it more indicative of a depositional event such as a flood or series of floods.

5.3. Tsunami horizons with correlation to previously identified events

The next anomaly identified, 'A2' (cal BP 3582to 3400, Table 1) resembles the previously identified and published sedimentary deposits from Caesarea (Fig. 8). The sedimentological character (fragmented and whole shell, pebbles, poorly sorted < 2000 μm grain size distribution) fits previously interpreted tsunamigenic horizons, and is chronologically similar with the timing of the Santorini eruption. Its presence here, as well as Caesarea, is expected given the far-field source and pan-eastern Mediterranean nature of the event. Following this deposit, a layer of non-tsunami sediments (49–59 cm) are followed by another shelly, poorly sorted anomaly (29–49 cm, 'A1', cal BP 1292 to 1169; Table 1, Fig. 8). An earthquake and possible tsunami is included in the catalogues around 748/749 CE (Amiran et al., 1994; Papadopoulos et al., 2014; Salamon et al., 2011), corresponding with this event.

There is an absence of certain tsunami events that are present in Caesarea, but not in Jisr al-Zarka (e.g. 2nd century AD tsunami,

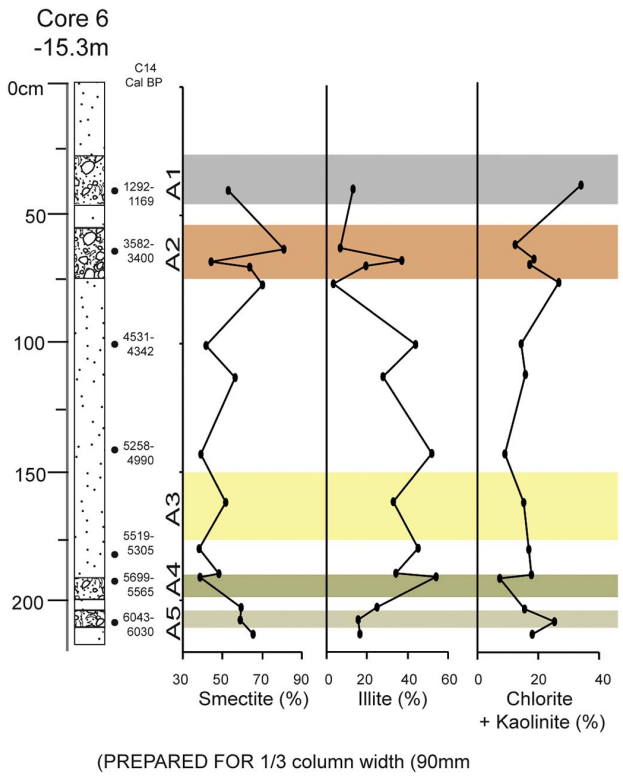

(PREPARED FOR 1/3 column width (90mm

Fig. 5. X-ray analysis, depicting results of clay minerals ratios estimations in core 6.

(Goodman-Tchernov et al., 2009; Reinhardt et al., 2006). This could be the result of erosion or remixing during later tsunamis (see discussion in Dey et al., 2014; Goodman-Tchernov and Austin, 2015) or more localized impacts associated with specific geomorphological features, as well as relative distance from source mechanisms. Storms or floods might have had an impact, although seabottom erosion from storms have yet to be documented at these depths in this area, and the lack of any banding or clear markers of regular, periodic flooding, are absent (except perhaps climate-associated anomaly A3). Caesarea is unique because of the presence of a large harbor for the past 2000 years, which can cause magnification of the wave when the tsunami wave enters the harbor (Kawai et al., 2014; Lynett et al., 2012) and alter the depositional potential of each tsunami (Goodman-Tchernov and Austin, 2015). Another consideration is of course, highly localized affects that might be reduced with a larger collection campaign. The results also do not confirm a 1759 tsunami, previously proposed based on the presence of liquefaction flame-features within the nearby reservoir (Marco et al., 2014) and an historical reference (Amiran et al., 1994).

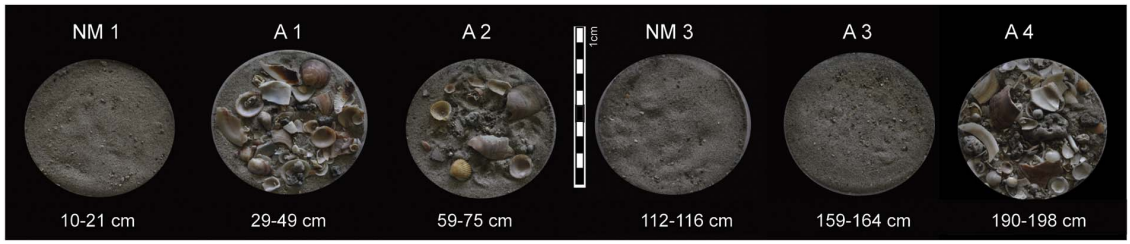

Fig. 4. Photographs of the sediments from core 6 demonstrate intervals from 'normal' marine (NM) and anomalous intervals (A).

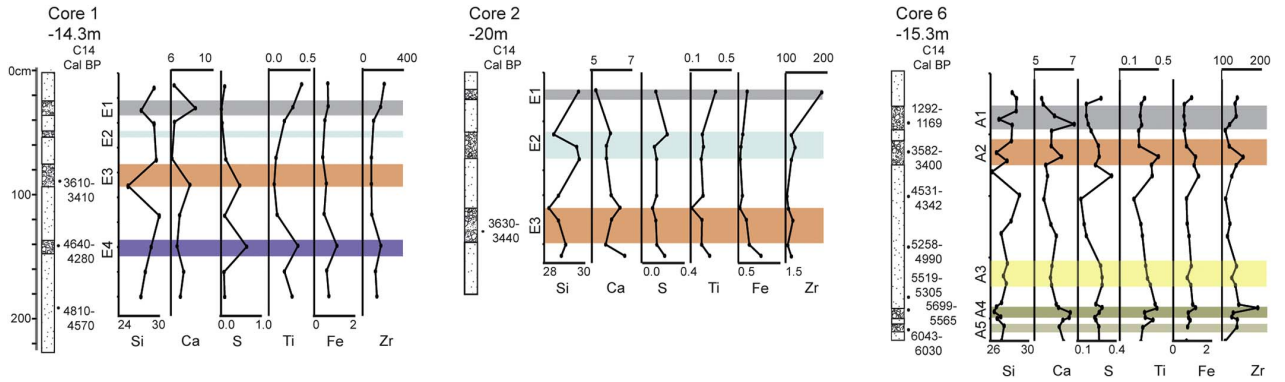

Fig. 6. Geochemical stratigraphy of cores 1, 2 and 6. Major elements (Si, Ca, S, Ti, Fe (%) and Zr (mg/g)) measured by XRF spectrometer.

5.4. Methodological efficacy and local considerations

XRF and XRD gave fair correlation for differentiating the anomalous deposits, but F-TIR did not give significant results. With any proxy, the local conditions are key to the efficacy of the analytical tools used. Here, the similarity between the composition of the eroding coastline (terrestrial) and the offshore input from further field sources could be the primary issue. The Nile was the predominant source of terrestrial sediment supply in the Levant Basin and its margins since the early Pliocene, and thus is responsible for both the more recently introduced sands as well as sands that make up the coastal aeolianite (Horowitz, 1979; Goldsmith and Golik, 1980; Zviely et al., 2007). Therefore, the mineralogical signal of the nearshore coastal sediments and the more recently introduced Nilotic sediments is similar. That is the mostly likely reason for the ambiguity of differentiating between terrestrially and marine-sourced sands for this area. For example, the conservative mode values (< 2000 μm), even within the anomalies, may be a reflection of the extreme dominance of this primary source. The studies of these clay minerals ratios in core 6 and a nearly pure clay comparative surface sample from 50 m water depth showed certain variations in which the higher terrestrial input was distinguishable in the suspected tsunamigenic horizons of the shallower core relative to deep sample.

Unfortunately, despite considerable efforts and repetition of analysis following questionable results, FT-IR did not provide clear linkages to tsunami horizons in proximal continental shelf samples. FT-IR is not widely present in tsunami sedimentological literature, though it has been recommended as a potential tool (Pongpiachan et al., 2013; Veerasingam et al., 2014). Following our work, we cannot endorse FT-IR as we applied it. It is possible that with newer systems or higher resolution it may be more informative. Despite our failure in this regard, we share our results in the hope of assisting others as they select their analytical approaches and establish their protocols.

Stages of tsunami waves have been divided into several phases; namely generation, propagation and inundation of the coastal areas, followed by traction and transport of terrestrial material into the marine environment by back channeling and other currents (Dawson and Stewart, 2007). During tsunamis and floods, canals of local rivers can be topographically favorable areas for terrestrial material to be transported to the basin (Scheucher and Vortisch, 2011). Sedimentary material from the Crocodile River consists of clays, silts, and also reworked nile-derived sands introduced during storms as well as eroded from the eolianite ridges. These sediments can be transported by backwash currents from the land following a tsunami event. However, in this area, these fine sediments do not stay for a long time on the seafloor, and rather are quickly dispersed by the waves and long-shore transport (Almagor, 2005). For example, following a rainy period that is accompanied by heavy river discharge, the shallow (< 20 m below mean sea level) waters will appear brown for a few days, but quickly clear and fine sediments are not observed on the sandy seafloor whatsoever. The absence of regular banding within the offshore sediments also suggests that the distinctive markers of these events do not preserve for the long duration. It was, however, determined that tsunami events were clearly identified at 10 to 20 m depth (Reinhardt et al., 2006; Goodman-Tchernov et al., 2009). Those cores and excavations,

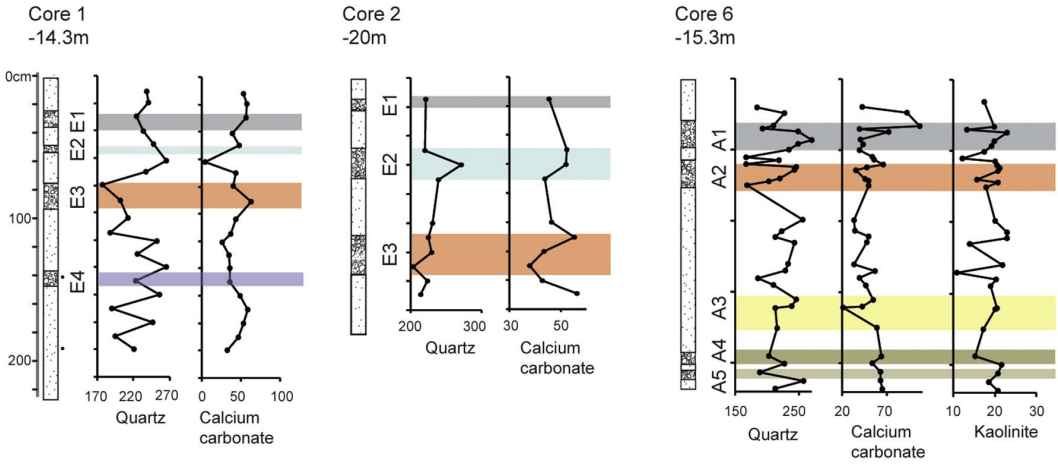

Fig. 7. Geochemical stratigraphy of cores 1, 2 and 6. Major sediment components (quartz and calcium carbonate) are expressed as relative ratios based on peaks areas calculations; kaolonite relative content variations are expressed in %. The parameters are measured by FT-IR Spectrometer.

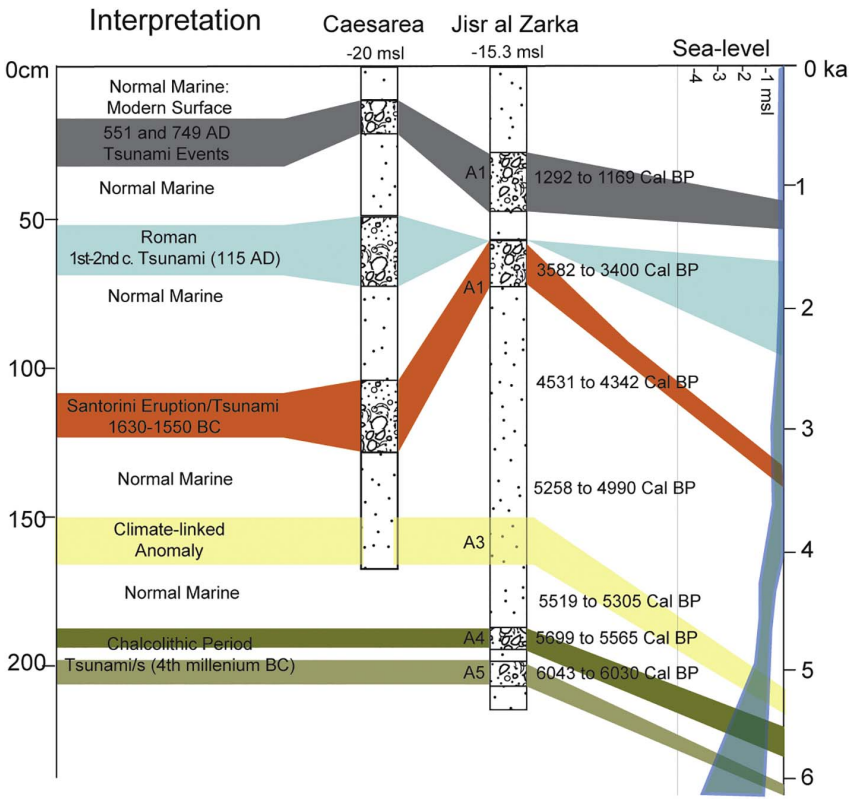

Fig. 8. Stratigraphic correlation of the core 6 offshore Jisr al-Zarka with representative core 2 (see Fig. 1) from Caesarea (adapted from Goodman-Tchernov et al., 2009). Sea level data are according to Sivan et al. (2001, 2004).

from 10 to 15 m below mean sea level bear thick anomalous sedimentary layers (up to 80 cm), which were identified as tsunami deposits. Thus, it can be suggested that terrestrial deposits can be preserved in sedimentary sequence. Shore landscape is not of less importance. Low relief topography and the presence of river channels can greatly influence the distance of landward inundation, and related quantity of terrestrial material that returns to the shelf (Srinivasalu et al., 2009).

6. Conclusions

Offshore of Jisr al-Zarka, a sediment core from 15 m below sea level revealed the preserved remains of at least four unique anomalous events. Two of those events correlate chronologically and sedimentologically with tsunami horizons previously identified offshore of Caesarea, possibly associated to events that occurred in 749 CE and 3.5 ka BP (Santorini eruption). An earlier anomalous horizon ('A3') does not fit the tsunamigenic criteria, but does correspond with the mid-Holocene period of sea-level stagnation and climatic transition. The oldest anomalous horizon matched tsunamigenic criteria and was dated to ~5.6 to 6.0 ka BP, which is within the Chalcolithic cultural period, and represents the oldest tsunami event recognized in this region.

Multiproxy analysis and description of sediments proved useful in this study for recognizing and differentiating between different types of anomalies. Amongst the techniques applied, traditional granulometry (< 2000 μm particle size distribution and maximum inclusion size) and identification of allochtonous inclusions (shell/beach pebbles) remained the most informative, reinforced by the XRF results. Continued efforts at testing and applying different techniques on offshore cores will improve the set of tools available for past tsunami identification.

References

Abrantes, F., Lebreiro, S., Rodrigues, T., Gil, I., Bartels-Jónsdóttir, H., Oliveira, P., Kissel, C., Grimalt, J.O., 2005. Shallow-marine sediment cores record climate variability and earthquake activity off Lisbon (Portugal) for the last 2000 years. Quat. Sci. Rev. 24, 2477–2494. http://dx.doi.org/10.1016/j.quascirev.2004.04.009.

Abrantes, F., Alt-Epping, U., Lebreiro, S., Voelker, A., Schneider, R., 2008. Sedimentological record of tsunamis on shallow-shelf areas: the case of the 1969 AD and 1755 AD tsunamis on the Portuguese shelf off Lisbon. Mar. Geol. 249, 283–293. http://dx.doi.org/10.1016/j.margeo.2007.12.004.

Almagor, G., 2005. The Mediterranean coast of Israel. In: GSI Rep. GSI/13/02, (in Hebrew).

Amiran, R., Arieh, E., Turcotte, T., 1994. Earthquakes in Israel and adjacent Areas: observations. Isr. Explor. J. 44, 260–305.

Avnaim-Katav, S., Agnon, A., Sivan, D., Almogi-Labin, A., 2016. Calcareous assemblages of the southeastern Mediterranean low-tide estuaries - seasonal dynamics and paleoenvironmental implications. J. Sea Res. 108, 30–49. http://dx.doi.org/10.1016/j.seares.2015.12.002.

Babu, N., Babu, D.S.S., Das, P.N.M., 2007. Impact of tsunami on texture and mineralogy of a major placer deposit in southwest coast of India. Environ. Geol. 52, 71–80. http://dx.doi.org/10.1007/s00254-006-0450-7.

Bar-Matthews, M., Ayalon, A., Kaufman, A., Wasserburg, G.J., 1999. The eastern Mediterranean paleoclimate as a reflection of regional events: Soreq cave, Israel. Earth Planet. Sci. Lett. 166, 85–95. http://dx.doi.org/10.1016/S0012-821X(98)00275-1.

van den Bergh, G.D., Boer, W., Haas, H. De, Weering, T.C.E. Van, 2003. Shallow Marine Tsunami Deposits in Teluk Banten (NW Java, Indonesia), Generated by the 1883 Krakatau Eruption. 197http://dx.doi.org/10.1016/S0025-3227(03)00088-4.

Bintanja, R., van de Wal, R.S.W., Oerlemans, J., 2005. Modelled atmospheric temperatures and global sea levels over the past million years. Nature 437, 125–128. http://dx.doi.org/10.1038/nature03975.

Biscaye, P.E., 1965. Mineralogy and sedimentation of recent Deep-Sea clay in the Atlantic Ocean and adjacent seas and oceans. Geol. Soc. Am. Bull. 76, 803–832.

Bondevik, S., Inge Svendsen, J., Mangerud, J., 1997. Tsunami sedimentary facies deposited by the Storegga tsunami in shallow marine basins and coastal lakes, western Norway. Sedimentology 44, 1115–1131. http://dx.doi.org/10.1046/j.1365-3091.1997.d01-63.x.

Boyle, J.F., 2000. Rapid elemental analysis of sediment samples by isotope source XRF. J. Paleolimnol. 23, 213–221. http://dx.doi.org/10.1023/A:1008053503694.

Cascalho, J., Costa, P., Dawson, S., Milne, F., Rocha, A., 2016. Heavy mineral assemblages of the Storegga tsunami deposit. Sediment. Geol. 334, 21–33.

Chagué-Goff, C., 2010. Chemical signatures of palaeotsunamis: a forgotten proxy? Mar. Geol. 271, 67–71. http://dx.doi.org/10.1016/j.margeo.2010.01.010.

Chagué-Goff, C., Andrew, A., Szczuciński, W., Goff, J., Nishimura, Y., 2012. Geochemical signatures up to the maximum inundation of the 2011 Tohoku-oki tsunami — implications for the 869AD Jogan and other palaeotsunamis. Sediment. Geol. 282, 65–77. http://dx.doi.org/10.1016/j.sedgeo.2012.05.021.

Clague, J.J., Bobrowsky, P.T., Hutchinson, I., 2000. A review of geological records of large tsunamis at Vancouver Island, British Columbia, and implications for hazard. Quat. Sci. Rev. 19, 849–863. http://dx.doi.org/10.1016/S0277-3791(99)00101-8.

Costa, P., Andrade, C., Freitas, M., Oliveira, M., Lopes, V., Dawson, A., Moreno, J., Fatela, F., Jouanneau, J.-M., 2012. A tsunami record in the sedimentary archive of the central Algarve coast, Portugal: characterizing sediment, reconstructing sources and inundation paths. The Holocene 22, 899–914. http://dx.doi.org/10.1177/0959683611434227.

Costa, P.J., Andrade, C., Cascalho, J., Dawson, A.G., Freitas, M.C., Paris, R., Dawson, S., 2015. Onshore tsunami sediment transport mechanisms inferred from heavy mineral assemblages. The Holocene 25, 795–809.

Dawson, A.G., Shi, S., 2000. Tsunami deposits. Pure Appl. Geophys. 157, 875–897. http://dx.doi.org/10.1007/s000240050010.

Dawson, A.G., Stewart, I., 2007. Tsunami deposits in the geological record. Sediment. Geol. 200, 166–183. http://dx.doi.org/10.1016/j.sedgeo.2007.01.002.

De Martini, P.M., Barbano, M.S., Smedile, A., Gerardi, F., Pantosti, D., Del Carlo, P., Pirrotta, C., 2010. A unique 4000year long geological record of multiple tsunami inundations in the Augusta bay (eastern Sicily, Italy). Mar. Geol. 276, 42–57. http://dx.doi.org/10.1016/j.margeo.2010.07.005.

De Menocal, P.B., 2001. Cultural responses to climate change during the late Holocene. Science 667–673.

Dey, H., Goodman-Tchernov, B., 2010. Tsunamis and the port of Caesarea Maritima over the longue dur{{}{é}{}}e: a geoarchaeological perspective. Tsunamis port Caesarea Maritima over longue dur{{}{é}{}}e a geoarchaeological perspect. J. Rom. Archaeol. 23, 265–284. http://dx.doi.org/10.1017/S1047759400002397.

Dey, H., Goodman-Tchernov, B., Sharvit, J., 2014. Archaeological evidence for the tsunami of January 18, 749 Islamic,: a chapter in the history of early Caesarea, Qaysariyah (Caesarea Maritima). J. Rom. Archaeol. 27, 357–373.

Emery, K., Bentor, Y., 1960. The continental shelf of Israel: Israel Ministry of Development. Geol. Surv. Bull. 26, 25–41.

Feldens, P., Schwarzer, K., Szczuciński, W., Stattegger, K., Sakuna, D., Somgpongchaiykul, P., 2009. Impact of 2004 tsunami on seafloor morphology and offshore sediments, Pakarang Cape, Thailand. Pol. J. Environ. Stud. 18, 63–68.

Feldens, P., Schwarzer, K., Sakuna, D., Szczuciński, W., 2012. Sediment distribution on the inner continental shelf off Khao Lak (Thailand) after the 2004 Indian Ocean tsunami. Earth Planets Space 64, 875–887. http://dx.doi.org/10.5047/eps.2011.09.001.

Font, E., Nascimento, C., Omira, R., Baptista, M.A., Silva, P.F., 2011. Erratum to identification of tsunami-induced deposits using numerical modeling and rock magnetism techniques: a study case of the 1755 Lisbon tsunami in Algarve, Portugal. [Physics of the earth and planetary interiors volume 182, issues 3-4, pages 187-198]. Phys. Earth Planet. Inter. 184, 106–117. http://dx.doi.org/10.1016/j.pepi.2010.10.006.

Frechen, M., Neber, A., Tsatskin, A., Boenigk, W., Ronen, A., 2004. Chronology of Pleistocene sedimentary cycles in the Carmel coastal plain of Israel. Quat. Int. 121, 41–52. http://dx.doi.org/10.1016/j.quaint.2004.01.022.

Galili, E., Weinstein-Evron, M., Hershkovitz, I., Gopher, A., Kislev, M., Lernau, O., Kolska-Horwitz, L., Lernaut, H., 1993. Atlit-yam: a prehistoric site on the sea floor off the Israeli coast. J. Field Archaeol. 20, 133–157. http://dx.doi.org/10.1179/jfa.1993.20.2.133.

Galili, E., Horwitz, L.K., Hershkovitz, I., Eshed, V., Salamon, A., Zviely, D., Weinstein-Evron, M., Greenfield, H., 2008. Comment on “Holocene tsunamis from Mount Etna and the fate of Israeli Neolithic communities” by Maria Teresa Pareschi, Enzo Boschi, and Massimiliano Favalli. Geophys. Res. Lett. 35, 10–12. http://dx.doi.org/10.1029/2008GL033445.

Garcia, S.G., Camazano, M.S., 1968. DIfferentiation of kaolinite from chlorite by treatment with dimethyl-suphoxide. Clay Miner. 7, 447–450.

Garfunkel, Z., 1998. Constrains on the origin and history of the eastern Mediterranean basin. Tectonophysics 298, 5–35. http://dx.doi.org/10.1016/S0040-1951(98)00176-0.

Gianfreda, F., Mastronuzzi, G., Sansò, P., 2001. Impact of historical tsunamis on a sandy coastal barrier: an example from the northern Gargano coast, southern Italy. Nat. Hazards Earth Syst. Sci. 1, 213–219. http://dx.doi.org/10.5194/nhess-1-213-2001.

Goff, J., Chagué-Goff, C., Nichol, S., Jaffe, B., Dominey-Howes, D., 2012. Progress in palaeotsunami research. Sediment. Geol. 243–244, 70–88. http://dx.doi.org/10.1016/j.sedgeo.2011.11.002.

Goldsmith, V., Golik, A., 1980. Sediment transport model of the southeastern Mediterranean coast. Mar. Geol. 37, 147–175.

Goodman Tchernov, B., Katz, T., Shaked, Y., Qupty, N., Kanari, M., Niemi, T., Agnon, A., 2016. Offshore evidence for an undocumented tsunami event in the “low risk” gulf of Aqaba-Eilat, northern Red Sea. PLoS One 11, e0145802. http://dx.doi.org/10.1371/journal.pone.0145802.

Goodman-Tchernov, B.N., Austin Jr., J., 2015. Deterioration of Israel's Caesarea Maritima's ancient harbor linked to repeated tsunami events identified in geophysical mapping of offshore stratigraphy. J. Archaeol. Sci. Rep. 444–454.

Goodman-Tchernov, B., Katz, O., 2016. Holocene-era submerged notches along the southern Levantine coastline: punctuated sea level rise? Quat. Int. 401, 17–27. http://dx.doi.org/10.1016/j.quaint.2015.10.107.

Goodman-Tchernov, B.N., Dey, H.W., Reinhardt, E.G., McCoy, F., Mart, Y., 2009. Tsunami waves generated by the Santorini eruption reached eastern Mediterranean shores. Geology 37, 943–946. http://dx.doi.org/10.1130/G25704A.1.

Goto, K., Chagué-Goff, C., Fujino, S., Goff, J., Jaffe, B., Nishimura, Y., Richmond, B., Sugawara, D., Szczuciński, W., Tappin, D.R., Witter, R.C., Yulianto, E., 2011. New insights of tsunami hazard from the 2011 Tohoku-oki event. Mar. Geol. 290, 46–50. http://dx.doi.org/10.1016/j.margeo.2011.10.004.

Goto, K., Chagué-goff, C., Goff, J., Jaffe, B., 2012. The future of tsunami research following the 2011 Tohoku-oki event. Sediment. Geol. 282, 1–13. http://dx.doi.org/10.1016/j.sedgeo.2012.08.003.

Hindson, R.A., Andrade, C., 1999. Sedimentation and hydrodynamic processes associated with the tsunami generated by the 1755 Lisbon earthquake. Quat. Int. 56, 27–38. http://dx.doi.org/10.1016/S1040-6182(98)00014-7.

Horowitz, A., 1979. The Quaternary of Israel. Academic Press, New York.

Hutchinson, I., Clague, J.J., Mathewes, R.W., 1997. Reconstructing the tsunami record on an emerging coast: a case study of Kanim Lake, Vancouver Island, British Columbia, Canada. J. Coast. Res. 13, 545–553. http://dx.doi.org/10.2307/4298646.

Ikehara, K., Irino, T., Usami, K., Jenkins, R., Omura, A., Ashi, J., 2014. Possible submarine tsunami deposits on the outer shelf of Sendai Bay, Japan resulting from the 2011 earthquake and tsunami off the Pacific coast of Tohoku. Mar. Geol. 358, 120–127. http://dx.doi.org/10.1016/j.margeo.2014.11.004.

Inbar, M., 2000. Episodes of flash floods and boulder transport in the upper Jordan River. IAHS Publ. 185–200.

Inman, D.L., Jenkins, S.A., 1984. The Nile littoral cell and man's impact on the coastal zone of the southeastern Mediterranean. Coast. Eng. Proc. 1600–1617.

Jaffe, B.E., Goto, K., Sugawara, D., Richmond, B.M., Fujino, S., Nishimura, Y., 2012. Flow speed estimated by inverse modeling of sandy tsunami deposits: results from the 11 March 2011 tsunami on the coastal plain near the Sendai Airport, Yuriage Sendai Airport transect area in figure 4. Sediment. Geol. 282, 90–109.

Jagodziński, R., Sternal, B., Szczuciński, W., Lorenc, S., 2009. Heavy Minerals in 2004 Tsunami Deposits on Kho Khao Island, Thailand. 18. pp. 103–110.

Katz, O., Mushkin, A., 2013. Characteristics of sea-cliff erosion induced by a strong winter storm in the eastern Mediterranean. Quat. Res. (United States) 80, 20–32. http://dx.doi.org/10.1016/j.yqres.2013.04.004.

Katz, T., Hinat, H., Eyal, G., Steiner, Z., Braun, Y., Shalev, S., Goodman-Tchernov, B.N., 2015. Desert flash floods form hyperpycnal flows in the coral-rich gulf of Aqaba, Red Sea. Earth Planet. Sci. Lett. 417 (417), 87–98.

Kawai, H., Satoh, M., Kawaguchi, K., Katsumi, S., 2014. 2010 Chile and 2011 Tohoku tsunami profiles measured by GPS buoys and coastal wave and tide gauges in a Nationwide Ocean wave information network for ports and harbors. J. Waterw. Port Coast. Ocean Eng. 140, 1–8.

Kitahashi, T., Jenkins, R.G., Nomaki, H., Shimanaga, M., Fujikura, K., Kojima, S., 2014. Effect of the 2011 Tohoku earthquake on deep-sea meiofaunal assemblages inhabiting the landward slope of the Japan trench. Mar. Geol. 358, 128–137. http://dx.doi.org/10.1016/j.margeo.2014.05.004.

Lamy, F., Arz, H.W., Bond, G.C., Bahr, A., Pätzold, J., 2006. Multicentennial-scale hydrological changes in the Black Sea and northern Red Sea during the Holocene and the Arctic/North Atlantic Oscillation. Paleoceanography 21 (1), 1–11. http://dx.doi.org/10.1029/2005PA001184.

Lichter, M., Klein, M., Zviely, D., 2011. Dynamic morphology of small south-eastern Mediterranean river mouths: a conceptual model. Earth Surf. Process. Landf. 36, 547–562. http://dx.doi.org/10.1002/esp.2077.

Löwemark, L., Chen, H.F., Yang, T.N., Kylander, M., Yu, E.F., Hsu, Y.W., Lee, T.Q., Song, S.R., Jarvis, S., 2011. Normalizing XRF-scanner data: a cautionary note on the interpretation of high-resolution records from organic-rich lakes. J. Asian Earth Sci. 40, 1250–1256. http://dx.doi.org/10.1016/j.jseaes.2010.06.002.

Lynett, P.J., Borrero, J.C., Weiss, R., Son, S., Greer, D., Renteria, W., 2012. Observations and modeling of tsunami-induced currents in ports and harbors. Earth Planet. Sci. Lett. 327–328, 68–74. http://dx.doi.org/10.1016/j.epsl.2012.02.002.

Magny, M., Haas, J.N., 2004. A major widespread climatic change around 5300 cal. yr BP at the time of the Alpine Iceman. J. Quat. Sci. 19 (5), 423–430. http://dx.doi.org/10.1002/jqs.850.

Mahaney, W.C., Allen, C.C.R., Pentlavalli, P., Kulakova, A., Young, J.M., Dirszowsky, R.W., West, A., Kelleher, B., Jordan, S., Pulleyblank, C., O'Reilly, S., Murphy, B.T., Lasberg, K., Somelar, P., Garneau, M., Finkelstein, S.A., Sobol, M.K., Kalm, V., Costa, P.J.M., Hancock, R.G.V., Hart, K.M., Tricart, P., Barendregt, R.W., Bunch, T.E., Milner, M.W., 2016. Biostratigraphic evidence relating to the age-old question of Hannibal's invasion of Italy, I: history and geological reconstruction. Archaeometry. http://dx.doi.org/10.1111/arcm.12231. (n/a-n/a).

Mamo, B., Strotz, L., Dominey-Howes, D., 2009. Tsunami sediments and their foraminiferal assemblages. Earth-Sci. Rev. 96, 263–278. http://dx.doi.org/10.1016/j.earscirev.2009.06.007.

Mangerud, J., 1972. Radiocarbon dating of marine shells including a discussion of the apparent age of recent shells from Norway. Boreas 1, 143–172. http://dx.doi.org/10.1111/j.1502-3885.1972.tb00147.x.

Marco, S., Katz, O., Dray, Y., 2014. Historical sand injections on the Mediterranean shore of Israel: evidence for liquefaction hazard. Nat. Hazards 1449–1459. http://dx.doi.org/10.1007/s11069-014-1249-6.

Mart, Y., Perecman, I., 1996. Caesarea: Unique evidence for faulting patterns and sea level fluctuations in the late Holocene. In: Raban, A., Holum, K.G. (Eds.), Caesarea Maritima; A Retrospective after Two Millennia. E. J. Brill, Leiden, pp. 3–24.

Martín-Puertas, C., Valero-Garcés, B.L., Mata, M.P., Moreno, A., Giralt, S., Martínez-Ruiz, F., Jiménez-Espejo, F., 2011. Geochemical processes in a Mediterranean Lake: a high-resolution study of the last 4,000 years in Zo??Ar Lake, southern Spain. J. Paleolimnol. 46, 405–421. http://dx.doi.org/10.1007/s10933-009-9373-0.

Milker, Y., Wilken, M., Schumann, J., Sakuna, D., Feldens, P., Schwarzer, K., Schmiedl, G., 2013. Sediment transport on the inner shelf off Khao Lak (Andaman Sea, Thailand) during the 2004 Indian Ocean tsunami and former storm events: evidence from foraminiferal transfer functions. Nat. Hazards Earth Syst. Sci. 13, 3113–3128. http://dx.doi.org/10.5194/nhess-13-3113-2013.

Minoura, K., Nakaya, S., Uchida, M., 1994. Tsunami deposits in a lacustrine sequence of

the Sanriku coast, northeast Japan. Sediment. Geol. 89, 25–31. http://dx.doi.org/10.1016/0037-0738(94)90081-7.

Minoura, K., Imamura, F., Kuran, U., Nakamura, T., Papadopoulos, G.A., Takahashi, T., 2000. Discovery of Minoan Tsunami Deposits. http://dx.doi.org/10.1130/0091-7613(2000)028<0059.

Nakamura, Y., Nishimura, Y., Putra, P.S., 2012. Local variation of inundation, sedimentary characteristics, and mineral assemblages of the 2011 Tohoku-oki tsunami on the Misawa coast, Aomori, Japan. Sediment. Geol. 282, 216–227. http://dx.doi.org/10.1016/j.sedgeo.2012.06.003.

Neev, D., Bakler, N., Emery, K.O., 1987. Mediterranean Coasts of Israel and Sinai: Holocene Tectonism from Geology, Geophysics, and Archaeology. Taylor and Francis, New York.

Papadopoulos, G.A., Gràcia, E., Urgeles, R., Sallares, V., De Martini, P.M., Pantosti, D., González, M., Yalciner, A.C., Mascle, J., Sakellariou, D., Salamon, A., Tinti, S., Karastathis, V., Fokaefs, A., Camerlenghi, A., Novikova, T., Papageorgiou, A., 2014. Historical and pre-historical tsunamis in the Mediterranean and its connected seas: geological signatures, generation mechanisms and coastal impacts. Mar. Geol. 354, 81–109. http://dx.doi.org/10.1016/j.margeo.2014.04.014.

Pareschi, M.T., Boschi, E., Favalli, M., 2007. Holocene tsunamis from Mount Etna and the fate of Israeli Neolithic communities. Geophys. Res. Lett. 34, 1–6. http://dx.doi.org/10.1029/2007GL030717.

Paris, R., Fournier, J., Poizot, E., Etienne, S., Morin, J., Lavigne, F., Wassmer, P., 2010. Boulder and fine sediment transport and deposition by the 2004 tsunami in Lhok Nga (western Banda Aceh, Sumatra, Indonesia): a coupled offshore-onshore model. Mar. Geol. 268, 43–54. http://dx.doi.org/10.1016/j.margeo.2009.10.011.

Perlin, A., Kit, E., 2002. Apparent roughness in wave–current flow: implication for coastal studies. J. Hydraul. Eng. 128, 729–741. http://dx.doi.org/10.1061/(ASCE).

Pierce, J.W., Siegel, F.R., 1969. Quantification in clay mineral studies of sediments and sedimentary rocks. J. Sediment. Petrol. 39, 187–193.

Pilarczyk, J.E., Reinhardt, E.G., 2012. Testing foraminiferal taphonomy as a tsunami indicator in a shallow arid system lagoon: Sur, Sultanate of Oman. Mar. Geol. 295–298, 128–136. http://dx.doi.org/10.1016/j.margeo.2011.12.002.

Pomerancblum, M., 1966. The distribution of heavy minerals and their hydraulic equivalents in sediments of the Mediterranean continental shelf of Israel. J. Sediment. Res. 36 (1).

Pongpiachan, S., Thumanu, K., Na Phatthalung, W., Tipmanee, D., Kanchai, P., Feldens, P., Schwarzer, K., 2013. Using Fourier transform infrared (FTIR) to characterize tsunami deposits in near-shore and coastal waters of Thailand. Int. J. Tsunami Soc. 20, 57–102.

Rahav, E., Paytan, A., Chien, C., Ovadia, G., Katz, T., Herut, B., 2016. The impact of atmospheric dry deposition associated microbes on the southeastern Mediterranean Sea surface water following an intense dust storme. Front. Mar. Sci. 3, 127. http://dx.doi.org/10.3389/fmars.2016.00127.

Reinhardt, E.G., Fitton, R.J., Schwarcz, H.P., 2003. Isotopic (Sr, O, C) indicators of salinity and taphonomy in marginal marine systems. J. Foraminifer. Res. 33 (3), 262–272. http://dx.doi.org/10.2113/33.3.262. (Jul).

Reinhardt, E.G., Goodman, B.N., Boyce, J.I., Lopez, G., Van Hengstum, P., Rink, W.J., Mart, Y., Raban, A., 2006. The tsunami of 13 December A.D. 115 and the destruction of Herod the Great's harbor at Caesarea Maritima, Israel. Geology 34, 1061–1064. http://dx.doi.org/10.1130/G22780A.1.

Rhodes, B., Tuttle, M., Horton, B., Doner, L., Kelsey, H., Nelson, A., Cisternas, M., 2006. Paleotsunami research. EOS Trans. Am. Geophys. Union 87, 205–209.

Sakuna, D., Szczuciński, W., Feldens, P., Schwarzer, K., Khokiattiwong, S., 2012. Sedimentary deposits left by the 2004 Indian Ocean tsunami on the inner continental shelf offshore of Khao Lak, Andaman Sea (Thailand). Earth Planets Space 64, 931–943. http://dx.doi.org/10.5047/eps.2011.08.010.

Sakuna-Schwartz, D., Feldens, P., Schwarzer, K., Khokiattiwong, S., Stattegger, K., 2015. Internal structure of event layers preserved on the Andaman Sea continental shelf, Thailand: tsunami vs. storm and flash-flood deposits. Nat. Hazards Earth Syst. Sci. 15, 1181–1199. http://dx.doi.org/10.5194/nhess-15-1181-2015.

Salamon, A., Rockwell, T., Guidoboni, E., Comastri, A., 2011. A critical evaluation of tsunami records reported for the Levant coast from the second millennium BCE to the present. Isr. J. Earth Sci. 58, 327–354.

Sandler, A., Herut, B., 2000. Composition of clays along the continental shelf off Israel: contribution of the Nile versus local sources. Mar. Geol. 167, 339–354. http://dx.doi.org/10.1016/S0025-3227(00)00021-9.

Sawai, Y., Fujii, Y., Fujiwara, O., Kamataki, T., Komatsubara, J., Okamura, Y., Satake, K., Shishikura, M., 2008. Marine incursions of the past 1500 years and evidence of tsunamis at Suijin-numa, a coastal lake facing the Japan trench. The Holocene 18, 517–528. http://dx.doi.org/10.1177/0959683608089206.

Scheucher, L.E.A., Vortisch, W., 2011. Sedimentological and geomorphological effects of the Sumatra-Andaman tsunami in the area of Khao Lak, southern Thailand. Environ. Earth Sci. 63, 785–796. http://dx.doi.org/10.1007/s12665-010-0750-9.

Shanmugam, G., 2012. Process-sedimentological challenges in distinguishing paleo-tsunami deposits. Nat. Hazards 63, 5–30. http://dx.doi.org/10.1007/s11069-011-9766-z.

Shapira, A., Hofstetter, A., 1993. Source parameters and scaling relationships of earthquakes in Israel. Tectonophysics 217, 217–226. http://dx.doi.org/10.1016/0040-1951(93)90005-5.

Sivan, D., Wdowinski, S., Lambeck, K., Galili, E., Raban, A., 2001. Holocene sea-level changes along the Mediterranean coast of Israel, based on archaeological observations and numerical model. Palaeogeogr. Palaeoclimatol. Palaeoecol. 167, 101–117. http://dx.doi.org/10.1016/S0031-0182(00)00234-0.

Sivan, D., Lambeck, K., Toueg, R., Raban, A., Porath, Y., Shirman, B., 2004. Ancient coastal wells of Caesarea Maritima, Israel, an indicator for relative sea level changes during the last 2000 years. Earth Planet. Sci. Lett. 222, 315–330. http://dx.doi.org/10.1016/j.epsl.2004.02.007.

Sivan, D., Potasman, M., Almogi-Labin, A., Bar-Yosef Mayer, D.E., Spanier, E., Boaretto, E., 2006. The Glycymeris query along the coast and shallow shelf of Israel, southeast Mediterranean. Palaeogeogr. Palaeoclimatol. Palaeoecol. 233, 134–148. http://dx.doi.org/10.1016/j.palaeo.2005.09.018.

Smedile, A., De Martini, P.M., Pantosti, D., 2012. Combining inland and offshore paleotsunamis evidence: the Augusta bay (eastern Sicily, Italy) case study. Nat. Hazards Earth Syst. Sci. 12, 2557–2567. http://dx.doi.org/10.5194/nhess-12-2557-2012.

Spiske, M., Piepenbreier, J., Benavente, C., Bahlburg, H., 2013. Preservation potential of tsunami deposits on arid siliciclastic coasts. Earth Sci. Rev. 126, 58–73. http://dx.doi.org/10.1016/j.earscirev.2013.07.009.

Srinivasalu, S., Rajeshwara Rao, N., Thangadurai, N., Jonathan, M.P., Roy, P.D., Ram Mohan, V., Saravanan, P., 2009. Characteristics of 2004 tsunami deposits of the northern Tamil Nadu coast, southeastern India. Bol. Soc. Geol. Mex. 61, 111–118.

Srinivasalu, S., Jonathan, M.P., Thangadurai, N., Ram-Mohan, V., 2010. A study on pre- and post-tsunami shallow deposits off SE coast of India from the 2004 Indian Ocean tsunami: a geochemical approach. Nat. Hazards 52, 391–401. http://dx.doi.org/10.1007/s11069-009-9385-0.

Stanley, D.J., Nir, Y., Galili, E., 1998. Clay mineral distributions to interpret Nile cell provenance and dispersal: III. Offshore margin between nile delta and northern Israel. J. Coast. Res. 14, 196–217. http://dx.doi.org/10.2307/4298770.

Stieglitz, R.R., 1998. A late byzantine reservoir and “Piscina” at Tel Tanninim. Isr. Explor. J. 48, 54–65.

Stuiver, M., Reimer, P.J., 1993. Extended 14C Data Base and revised CALIB 3.0 14C age calibration program. Radiocarbon 35, 215–230.

Szczuciński, W., 2012. The post-depositional changes of the onshore 2004 tsunami deposits on the Andaman Sea coast of Thailand. Nat. Hazards 60, 115–133. http://dx.doi.org/10.1007/s11069-011-9956-8.

Tipmanee, D., Deelaman, W., Pongpiachan, S., Schwarzer, K., Sompongchaiyakul, P., 2012. Using polycyclic aromatic hydrocarbons (PAHs) as a chemical proxy to indicate tsunami 2004 backwash in Khao Lak coastal area, Thailand. Nat. Hazards Earth Syst. Sci. 12, 1441–1451. http://dx.doi.org/10.5194/nhess-12-1441-2012.

Udden, J.A., 1914. Mechanical composition of clastic sediments. Geol. Soc. Am. Bull. 25 (1), 655–744.

Veerasingam, S., Venkatachalapathy, R., Basavaiah, N., Ramkumar, T., Venkatramanan, S., Deenadayalan, K., 2014. Identification and characterization of tsunami deposits off southeast coast of India from the 2004 Indian Ocean tsunami: rock magnetic and geochemical approach. J. Earth Syst. Sci. 123, 905–921. http://dx.doi.org/10.1007/s12040-014-0427-y.

Venkatarathnam, K., Ryan, W., 1971. Dispersal patterns of clay minerals in the sediments of the eastern Mediterranean Sea. Mar. Geol. 11, 261–282.

Weiss, R., Bahlburg, H., 2006. A note on the preservation of offshore tsunami deposits. J. Sediment. Res. 76, 1267–1273. http://dx.doi.org/10.2110/jsr.2006.110.

Wentworth, C.K., 1922. A scale of grade and class terms for clastic sediments. J. Geol. 30 (5), 377–392.

Young, R.W., White, K.L., Price, D.M., 1996. Fluvial deposition on the Shoalhaven deltaic plain, southern new South Wales. Aust. Geogr. 27, 215–234. http://dx.doi.org/10.1080/00049189608703169.

Zviely, D., Kit, E., Klein, M., 2007. Longshore sand transport estimates along the Mediterranean coast of Israel in the Holocene. Mar. Geol. 238, 61–73. http://dx.doi.org/10.1016/j.margeo.2006.12.003.